Theoretical and experimental investigation of the triple-differential cross sections for electron-impact ionization of Kr(4*p*) and Xe(5*p*) at 1-keV impact energy

J. Rasch
Department of Applied Mathematics and Theoretical Physics, University of Cambridge, Silver Street, Cambridge CB3 9EW, England

M. Zitnik
J. Stefan Institute, University of Ljubljana, Ljubljana, Slovenia

L. Avaldi
Istituto Metodologie Avanzate Inorganiche, Consiglio Nationale delle Ricerche, Area della Ricerca di Roma, Via Salaria km 29300, C.P. CP10, 00016 Monterotondo Scalo, Roma, Italy

Colm T. Whelan
Department of Applied Mathematics and Theoretical Physics, University of Cambridge, Silver Street, Cambridge CB3 9EW, England

G. Stefani and R. Camilloni
Istituto Metodologie Avanzate Inorganiche, Consiglio Nationale delle Richerche, Area della Ricerca di Roma, Via Salaria km 29300, C.P. Box 10, 00016 Monterotondo Scalo, Roma, Italy

R. J. Allan
Department for Computation and Information, CCLRC Daresbury Laboratory, Warrington WA4 4AD, England

H. R. J. Walters
Department of Applied Mathematics and Theoretical Physics, The Queen's University of Belfast, Belfast BT7 1NN, Northern Ireland
(Received 10 June 1997)

The triple-differential cross sections for the ionization of Kr($4p$) and Xe($5p$) by a fast electron where the exiting electrons have energies of 20 eV and 1 keV have been measured and compared with distorted-wave Born calculations. Difficulties were encountered when trying to place the relative data on an absolute scale by extrapolation to the optical limit: an extensive study of this normalization process is presented and it is argued that it is not applicable to the heavier atoms considered here, but can be used effectively for helium targets. [S1050-2947(97)00112-1]

PACS number(s): 34.80.Dp

I. INTRODUCTION AND EXPERIMENTAL METHOD

Electron-electron coincidence experiments, usually known as $(e,2e)$ experiments, are the most powerful tool to study the process of electron-impact ionization [1,2]. Despite the extended activity in the field in the last years, the understanding of the process for targets heavier than H and He still presents many serious challenges for both theoreticians and experimentalists alike. As far as the experiments are concerned, the challenge consists in (a) providing a large body of experimental data to explore the various zones of the Bethe surface [3], and (b) determining the absolute scale of the triple-differential cross section (TDCS).

In this work we report a set of TDCS for the ionization of krypton ($4p$) and xenon ($5p$) orbitals where the incident electron had energies of 1034.5 and 1032.8 eV and in both cases one of the exiting electrons had an energy of 20 eV. We consider a number of scattering angles for the fast electron. The smaller this angle is the closer one comes to vanishing momentum transfer; in the limit of zero-momentum transfer the electron-impact ionization should go over to the photoionization cross section [4]. There is extensive experimental and theoretical information available in these highly asymmetric cases for hydrogen and helium (see [5,1]). In this paper we present a theoretical and experimental study of the TDCS for the heavier noble gases and we will show that the methods used for hydrogen and helium cannot be used to place these cross sections on an absolute scale.

There have been several proposed ways of normalizing the relative TDCS (for a review see [6]). A direct way to determine the absolute scale would be to use the relationship [6]

$$\frac{d^3\sigma}{d\Omega_1 d\Omega_2 dE} = \frac{I_c}{I_0}\frac{1}{nl(\epsilon_1\Delta\Omega_1)(\epsilon_2\Delta\Omega_2)\Delta E_c}, \qquad (1)$$

where I_c is the coincidence count rate, I_0 the incident electron rate, l the effective overlap length of the gas and electron beam, n the target density, $\Delta\Omega_1$ and $\Delta\Omega_2$ the acceptance solid angles of the analyzers, ΔE_c the effective coincidence energy resolution, and ϵ_1 and ϵ_2 the overall detection efficiencies of the analyzers. Unfortunately, most of these quantities are rather difficult to determine [7,8]. Other techniques have been considered. Among the other proce-

dures [6] we will consider the normalization procedure that was first used by Jung *et al.* [9] to put their helium data taken at an impact energy of 600 eV onto an absolute scale. It exploits the optical properties of the target and its cross sections, for inelastic electron scattering, and is one of the most widely used methods. In Sec. II we will describe the experimental setup and the normalization procedure and outline the relation between the TDCS and its optical limit. Section III will be devoted to the theoretical method, while in Sec. IV experimental and theoretical results are compared.

The normalization procedure leads to cross-section values that are larger than the predicted theoretical results. A detailed study of the possible source of this discrepancy is presented, possible numerical faults in the calculation are considered, but eliminated, and it is shown that the normalization procedure fails due to the very strong distorting effects of the heavy nuclei. The same analysis is applied to the earlier helium data and it is shown that the extrapolation technique is valid in that case. The principal consequence of this study is that we have demonstrated that the extrapolation technique does not offer a viable method for placing experimental data for the heavier atoms onto an absolute scale.

II. EXPERIMENT AND LIMITING PROCEDURE

A. Experimental setup

The apparatus used for the present measurements is an electron-impact spectrometer specially designed for the electron coincidence experiments. It consists of a vacuum chamber that contains an electron-beam source, two electrostatic hemispherical analyzers, and an effusive gaseous beam. A complete description of the apparatus is reported elsewhere [10,11]. Here only the details relevant to the present measurements are repeated. The present measurements were performed at an incident energy E_0 of about 1000 eV with an incident-beam current around 0.5μA. The electrons that are either inelastically scattered or ejected by the target into a cone around the direction ϑ with respect to the incident beam are analyzed in energy by passing through one of the two electron spectrometers, independently movable in the scattering plane from $-15°$ to 150° with a precision of 0.1°. The angular acceptances of the analyzers in the present measurements were set to $\pm 0.5°$ and $\pm 4°$ for the scattered (labeled 1 in the following) and ejected (labeled 2) electron analyzers, respectively.

The full width half maximum (FWHM) energy resolutions of the analyzers, operated at a constant pass energy (E_p=100 eV), where $\Delta E_1 = \Delta E_2 = 1.1$ eV resulting in an overall energy resolution of ≈ 1.6 eV when measuring the energy separation spectra and of ≈ 0.8 eV when measuring the angular distributions [7,12]. The uncertainty in the magnitude and direction of the momentum transfer, $\boldsymbol{K} := \boldsymbol{k}_0 - \boldsymbol{k}_1$, derived from the quoted experimental energy and angular acceptances *assuming the two contributions are uncorrelated*, are strongly dependent on the kinematics investigated. In the worst case they can be as large ± 0.1 a.u. and $\pm 8°$ (see Table I). The coincidence measurements reported in this paper were collected in the asymmetric regime, i.e., $E_1 \gg E_2$. Energies E_1 and E_2 were kept fixed at 1000 and 20 eV, respectively. The measurements have been performed by collecting the scattered electrons at a fixed angle ϑ_1, while the ejected electron angle ϑ_2 was varied from 35° to 150°.

TABLE I. Shown are the direction and magnitude of the momentum transfer $\boldsymbol{K} := \boldsymbol{k}_0 - \boldsymbol{k}_1$, derived from the quoted experimental energy and angular acceptances.

	Kr $(4p)$	Kr $(4p)$	Xe $(5p)$	Xe $(5p)$
ϑ_1 [°]	2.0	8.0	2.5	8.0
K [a.u.]	0.33 ± 0.1	1.22 ± 0.1	0.40 ± 0.1	1.20 ± 0.1
$\vartheta_{\boldsymbol{K}}$ [deg]	63.2 ± 8	77.1 ± 0.7	68.5 ± 5.3	79.4 ± 0.7

The collection efficiency of the ejected-electron analyzer has been calibrated on He by measuring the double-differential cross section (DDCS) $d^2\sigma/d\Omega_2 dE$, for energies for the ejected electrons equal to the ones actually collected in the $(e,2e)$ experiments. The shapes of the measured DDCS's are in good agreement with the ones ''recommended'' by Kim [13] at 20-eV ejected electron energy. The zero of the scattered angle scale was set by determining the symmetry of the scattered electron DDCS. The full set of kinematics investigated in the present paper is reported in Table I.

The typical coincidence rate was a few per second on the maximum of the TDCS where the true-to-random coincidence ratio was roughly equal to one. In the worst case, i.e., in Kr at $\vartheta_1 = 8°$, $\vartheta_2 \approx 300°$ the coincidence count rate was 0.1 per second and the true-to-random coincidence ratio 0.1.

B. The limiting procedure

The method of Jung *et al.* [9] is based on work by Lassettre *et al.* and Inokuti [3,14] who found that in the limit of zero-momentum transfer higher-order effects tend to zero at any given energy so that a first Born treatment of the scattering problem becomes justified. In this case it is then possible to show that the triple differential generalized oscillator strength (GOS) is proportional to the optical oscillator strength (OOS)

$$\int \left(\lim_{K \to 0} \frac{d^3 \overline{f}(K)}{d\Omega_2 d\Omega_K dE} \right) d\Omega_K = \frac{d \overline{f}_{\rm opt}}{d\Omega_2 dE}, \tag{2}$$

where the double-differential GOS and the OOS are defined as

$$\frac{d^3 \overline{f}}{d\Omega_2 d\Omega_K dE} := 2 \frac{E_2 - E_b}{K^2} \sum_{m_b} \left| \int \chi_b^-(\boldsymbol{r}_2) e^{i \boldsymbol{K} \cdot \boldsymbol{r}_2} \phi_{m_b}(\boldsymbol{r}_2) d\boldsymbol{r}_2 \right|^2, \tag{3}$$

$$\frac{d^2 \overline{f}_{\rm opt}}{d\Omega_2 dE} := \frac{2}{3} (E_2 - E_b) \sum_{m_b} \left| \int \chi_2(\boldsymbol{r}_2) \boldsymbol{r}_2 \phi_{m_b}(\boldsymbol{r}_2) d\boldsymbol{r}_2 \right|^2. \tag{4}$$

It should be noted, however, that in the case of hydrogen and helium we are ionizing an *s* state. This means that we do not have to deal with degenerate magnetic sublevels. In the krypton $(4p)$ and xenon $(5p)$ experiment the gas target consisted of unpolarized atoms so that no distinction between different sublevels has been made. We therefore have to av-

erage over the magnetic sublevels m_b. Barred quantities will always denote such an average.

Making use of a first Born treatment the TDCS can be related to the GOS equation (3) in the form

$$\frac{d^3\overline{\sigma}}{d\Omega_1 d\Omega_2 dE}=2\frac{k_1k_2}{k_0}\frac{1}{K^2}\frac{1}{(E_2-E_b)}\frac{d^3\overline{f}}{d\Omega_2 d\Omega_K dE}. \quad (5)$$

It can furthermore be shown that (see [15])

$$\lim_{K\to 0}\frac{d^3\overline{f}}{d\Omega_2 d\Omega_K dE}=\frac{1}{8\pi^3\alpha k_2}\frac{d\overline{\sigma}}{dE}[1+\beta P_2(\hat{\boldsymbol{k}}_2\cdot\hat{\boldsymbol{K}})] \quad (6)$$

so that we get for the limit of the TDCS

$$\lim_{K\to 0}K^2\frac{d^3\overline{\sigma}}{d\Omega_1 d\Omega_2 dE}=\frac{1}{4\pi^3\alpha}\frac{k_1}{k_0}\frac{1}{(E_2-E_b)}\times\frac{d\overline{\sigma}}{dE}[1+\beta P_2(\hat{\boldsymbol{k}}_2\cdot\hat{\boldsymbol{K}})]. \quad (7)$$

In Eqs. (6) and (7) $d\overline{\sigma}/dE$ and β are the photoionization cross section and the asymmetry parameter, respectively. P_2 is a Legendre polynomial of the first kind. It should be noted that the value of β depends of course on the target subshell. For an s state we get the well-known result $\beta=2$. In the case of a p state the result is more complicated (see [15]).

From Eq. (7) it follows directly that the TDCS measured in the direction $\boldsymbol{k}_2\| \boldsymbol{K}$ and $\boldsymbol{k}_2\| -\boldsymbol{K}$ multiplied by K^2 tends to the same value

$$\sigma_{\lim}:=\lim_{K\to 0}K^2\frac{d^3\overline{\sigma}}{d\Omega_1 d\Omega_2 dE}=\frac{1}{4\pi^3\alpha}\frac{k_1}{k_0}\frac{1}{(E_2-E_b)}\frac{d\overline{\sigma}}{dE}[1+\beta] \quad (8)$$

when K vanishes. Therefore the value of this limit is known from the kinematics of experiment and photoionization data.

The limit itself can physically not be reached because of the ionization threshold. To get information on the limit one has to measure the coincidence yield in the direction $\boldsymbol{k}_2\| \boldsymbol{K}$ for several values of ϑ_1, i.e., for several values of $\boldsymbol{K}$. One obtains two curves that have to join in the limit so that by extrapolating the two curves across the unphysical region we get the cross section for the point of zero-momentum transfer. In the present work we have measured the relative TDCS at several ϑ_1's between 1° and 8° . The minimum momentum transfer K measured was 0.21 and 0.26 a.u. in Kr and Xe, respectively.

In order to extrapolate the experimental data to the optical limit we have, in all cases, used a standard general linear least-squares fitting routine, which can be found in, e.g., in [16]. It has the advantage that one cannot only choose the order of the polynomials but also by ''freezing'' the parameters of the fitting polynomial one can choose whether only even or odd or a combination of both should be used. Klar *et al.* [17] studied the structure of the form factor

$$\overline{\epsilon}:=\sum_{m_b}\left|\int\chi_b^-(\boldsymbol{r}_2)e^{i\boldsymbol{K}\cdot\boldsymbol{r}_2}\phi_{m_b}(\boldsymbol{r}_2)d\boldsymbol{r}_2\right|^2 \quad (9)$$

in more detail to give supplementary limitations to the extrapolation. In particular in the optical limit the expansion of the optical oscillator strength should only contain even powers of K. The problems inherent in the extrapolation method will be discussed in some detail below.

III. DISTORTED-WAVE BORN APPROXIMATION (DWBA)

The TDCS for closed shell atoms is of the form [2,15]

$$\frac{d^3\overline{\sigma}}{d\Omega_1 d\Omega_2 dE}=(2\pi)^4\frac{k_1k_2}{k_0}\times\sum_{m_b}[|f_{m_b}-g_{m_b}|^2+|g_{m_b}|^2+|f_{m_b}|^2], \quad (10)$$

where

$$f_{m_b}=\int\int\chi_a^-(\boldsymbol{k}_1,\boldsymbol{r}_1)\chi_b^-(\boldsymbol{k}_2,\boldsymbol{r}_2)\times\frac{1}{|\boldsymbol{r}_1-\boldsymbol{r}_2|}\chi_i^+(\boldsymbol{k}_0,\boldsymbol{r}_1)\phi_{m_b}(\boldsymbol{r}_2)d\boldsymbol{r}_1d\boldsymbol{r}_2, \quad (11)$$

$$g_{m_b}=\int\int\chi_a^-(\boldsymbol{k}_1,\boldsymbol{r}_2)\chi_b^-(\boldsymbol{k}_2,\boldsymbol{r}_1)\times\frac{1}{|\boldsymbol{r}_1-\boldsymbol{r}_2|}\chi_i^+(\boldsymbol{k}_0,\boldsymbol{r}_2)\phi_{m_b}(\boldsymbol{r}_1)d\boldsymbol{r}_1d\boldsymbol{r}_2. \quad (12)$$

$\chi_i^+(\boldsymbol{k}_0,\boldsymbol{r}_1)$ denotes the distorted wave representing the incoming electron calculated in the triplet local exchange potential of the atom whereas $\chi_a^-(\boldsymbol{k}_1,\boldsymbol{r}_1)$ and $\chi_b^-(\boldsymbol{k}_2,\boldsymbol{r}_2)$ are the distorted waves calculated in the triplet exchange potential of the atom for the fast electron (label 1) and ion for the slow outgoing electron (label 2).

We use a triplet exchange potential of Furness-McCarthy type (see [2,15,18]). In the case considered here where E_2, the energy of the slow outgoing electron, is comparable to the energy of the target bound state one should expect the exchange to be important in the elastic channels. In fact our calculations showed that the exchange potential is extremely important in this case [15]. It should, however, be noted that the exchange amplitude g that we include in our calculation should be negligible compared with the direct amplitude f. In fact our calculation showed that the exchange amplitude contributed on average not more than about 1–2% to the overall cross section.

In order to account for and test the significance of the electron-electron repulsion we multiplied the pure DWBA cross section equation (10) by an M_{ee} factor of Ward and Macek [19]. These authors suggested this factor to model the repulsion effects of the two outgoing electrons. It retains the normalization of the DWBA and exhibits the correct Wannier threshold law in the zero-energy limit in contrast to the N_{ee} factor as used in [20] and [21], which does not have

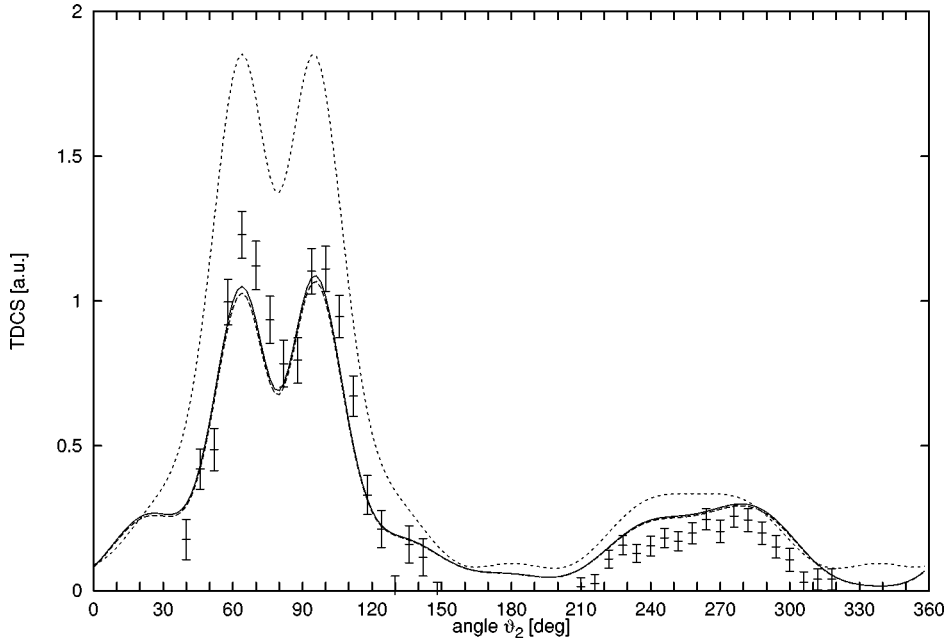

FIG. 1. TDCS of xenon $(5p)$ at an impact energy of 1032.8 eV, energy of slow outgoing electron is 20 eV, fast electron fixed at an angle of $\vartheta_1=8°$. Experimental data scaled to give the best fit to the theory. Shown are DWBA (solid line), DWBA multiplied with the M_{ee} factor (long dashed), and first Born calculation (short dashed).

these properties but is very similar in shape. As expected the M_{ee} factor makes hardly any difference in this geometry (see Figs. 1–4).

IV. COMPARISON OF EXPERIMENT AND THEORY

In the Figs. 1–4 we compare theoretical and experimental results. Shown are a first Born calculation, the DWBA, and the DWBA multiplied with the M_{ee} factor (see [19]).

A. Shape agreement

The data $\vartheta_1=8°$ on the Bethe ridge in Figs. 1 and 3 are characterized by a split in the binary lobe with the minimum in the direction of the momentum transfer. This is typical for a p-state target. We note that in the case of xenon we have a nonvanishing coincidence yield in the backward direction and for krypton a recoil lobe has been observed but with a lower intensity than in xenon. No appreciable shift of the symmetry of the experimental TDCS from the direction of K has been observed in this kinematics. If we now compare

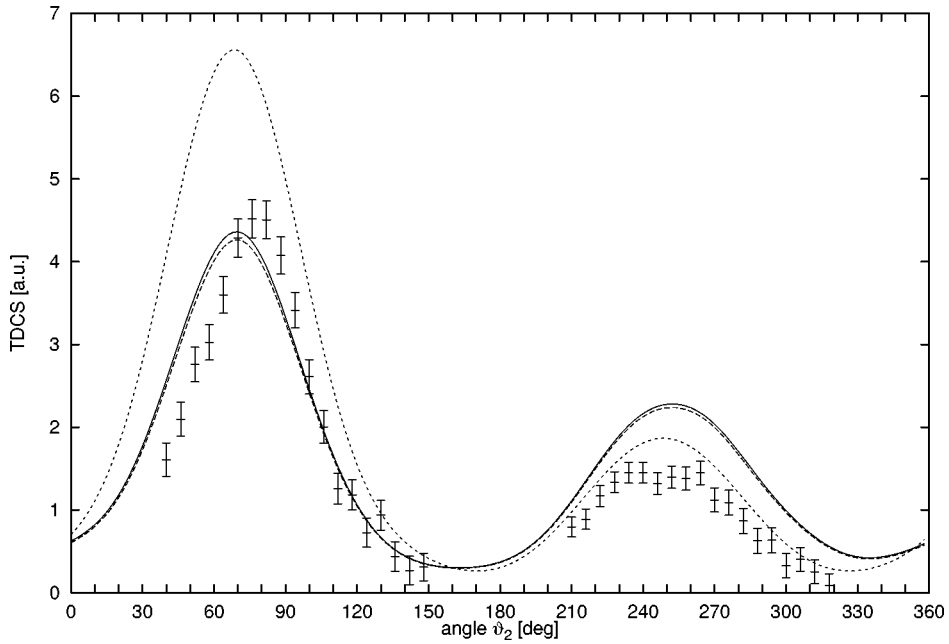

FIG. 2. TDCS of xenon $(5p)$ at an impact energy of 1032.8 eV, energy of slow outgoing electron is 20 eV, fast electron fixed at an angle of $\vartheta_1=2°$. Experimental data scaled to give the best fit to the theory. Shown are DWBA (solid line), DWBA multiplied with the M_{ee} factor (long dashed), and first Born calculation (short dashed).

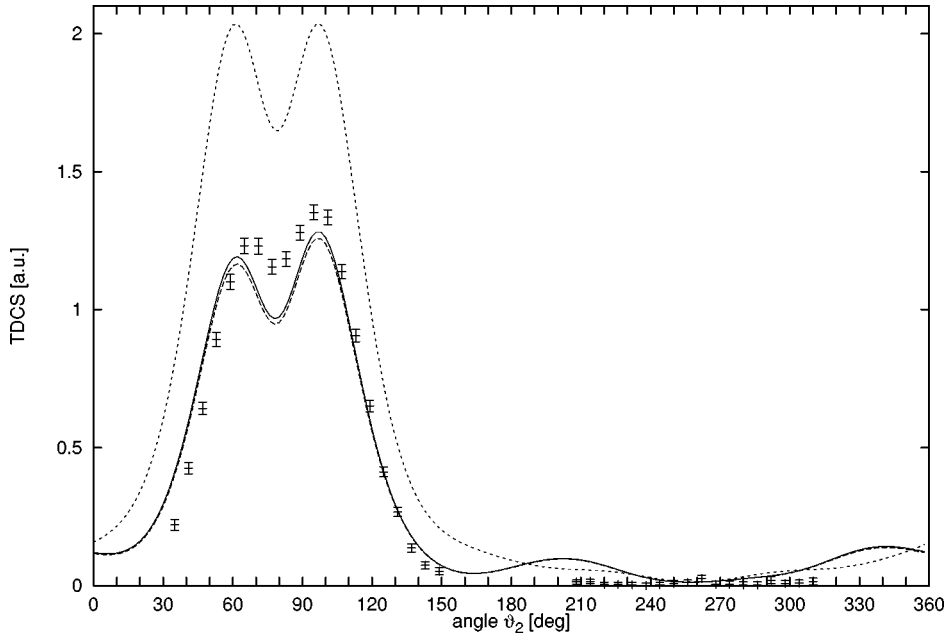

FIG. 3. TDCS of krypton ($4p$) at an impact energy of 1034.5 eV, energy of slow outgoing electron is 20 eV, fast electron fixed at an angle of $\vartheta_1=8°$. Experimental data scaled to give the best fit to the theory. Shown are DWBA (solid line), DWBA multiplied with the M_{ee} factor (long dashed), and first Born calculation (short dashed).

experiment and theory we find that the overall shape agreement is good. Especially in the binary region and for larger scattering angles of the fast outgoing electron ($\vartheta_1=8°$ for krypton and xenon) we get very good shape agreement with experiment. This is also the region where the first Born does rather poorly. We note that for both krypton and xenon at smaller scattering angles there is an indication of a slightshift of the binary maximum away from the direction of momentum transfer. A similar shift has been observed in the case of hydrogen and helium and is best explained in terms of postcollisional interaction between the exiting electrons (see [2,22,23,24]). Here we note, however, that the apparent rotation of the binary peak away from the scattered electron beam is not given theoretically even when we include final channel postcollisional interactions (PCI) through the M_{ee} factor. The effect is very small and the overall shape agreement between theory and experiment is excellent; only in the recoil direction do we get some deviation.

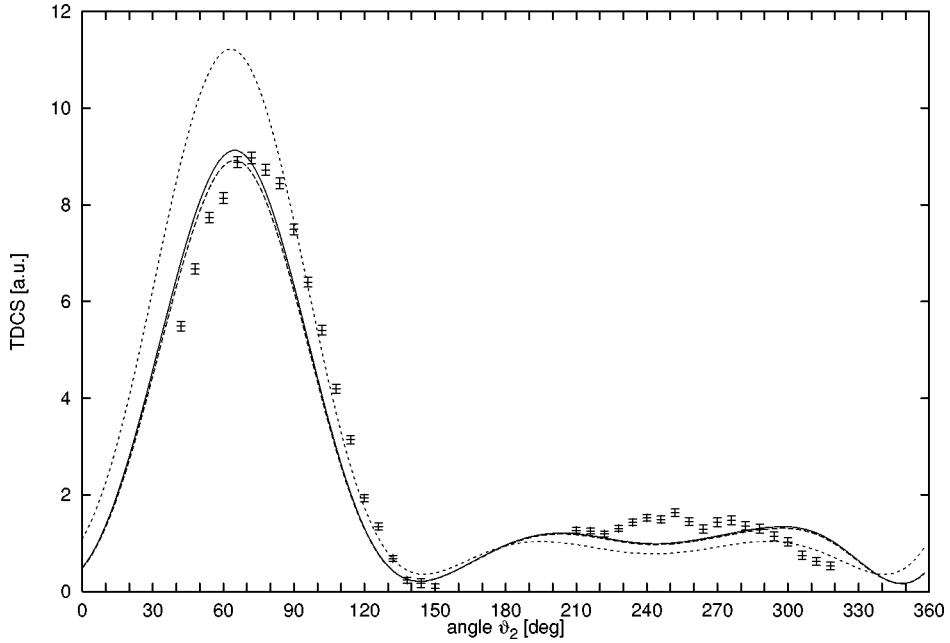

FIG. 4. TDCS of krypton ($4p$) at an impact energy of 1034.5 eV, energy of slow outgoing electron is 20 eV, fast electron fixed at an angle of $\vartheta_1=2°$. Experimental data scaled to give the best fit to the theory. Shown are DWBA (solid line), DWBA multiplied with the M_{ee} factor (long dashed), and first Born calculation (short dashed).

TABLE II. Comparison of the values for β determined experimentally and from the DWBA calculation using different forms of the local exchange potential for the slow outgoing electron. $\omega = E_2 - E_b$ denotes the energy difference.

	Kr $(4p)$	Xe $(5p)$
ω (eV)	34.5	32.8
β exp.	1.85 ± 0.1 [28]	1.73 ± 0.07 [27]
β DWBA	1.85	1.72

B. Absolute scale

We have attempted to apply the same technique as Jung *et al.* [9] to place the data on an absolute scale. To this end the TDCS's in the $\boldsymbol{K}$ and $-\boldsymbol{K}$ directions have been measured from $\theta_1 = 1°$ to 8°. The details of the fitting procedure will be dealt with in Sec. VI. The experimental values of σ and β shown in Tables II and III at the required energy loss were derived from the partial photoionization cross sections [25,26] and the photoionization angular measurements of [27,28]. The overall uncertainty on the absolute scale is about 28%, due to the uncertainty in the σ of 17% and 9% and in the β of 5% and 4% for Kr $(4p)$ and Xe $(5p)$, respectively. As we shall see below the application of this method produces a large discrepancy between our DWBA calculations and the normalized experimental data for xenon and krypton, but agreement in absolute size with the helium data of Jung *et al.* [9] is very good. In the case of krypton $(4p)$ and xenon $(5p)$, however, we had to rescale the experimental data to get the best fit to the theory. In particular in Figs. 1 and 2 the experimental data are downscaled by a factor of 3.5 while for Kr in Figs. 3 and 4 it is downscaled by a factor of 6.6 and 4.3, respectively. Thus the question arises: what is going wrong? In the following we will elucidate this question by first concentrating on theoretical problems. We will then show that the normalization works very well for helium and then describe the problems that arise for Kr and Xe. The details of the fitting procedure will be dealt with in Sec. VI.

V. WHAT CAN GO WRONG THEORETICALLY?

On the theoretical side there are two main problems that can arise. In very asymmetric geometry getting the TDCS to converge is a highly nontrivial problem. The mathematical problems encountered in the calculation and how they have been tackled is explained in great detail in [15]. In Sec. V A we will merely summarize the results.

TABLE III. Comparison of the values for σ determined experimentally and from the DWBA calculation using different forms of the local exchange potential for the slow outgoing electron. $\omega = E_2 - E_b$ denotes the energy difference.

	Kr $(4p)$	Xe $(5p)$
ω (eV)	34.5	32.8
σ Expt.	11.6 ± 2.0 [26]	4.40 ± 0.4 [25]
σ DWBA	4.26	3.96

A. Convergence of the DWBA calculation

While the very asymmetric geometry of the scattering event makes it possible to normalize the cross section it imposes a severe problem on the theory. In this geometry it is clear that the contribution from higher-order effects such as postcollisional interactions (e-e repulsion) and polarization will contribute very little. However, even neglecting these effects, we have to face a convergence problem introduced by the slowly vanishing overlap integrals. These overlap integrals between the fast incoming and fast outgoing electron tend to go to zero very slowly for high l values. This can very easily be seen as follows. The radial Born integrals we have to solve are of the form

$$I_{\mathrm{Born}}(l_1,l_2,\lambda,l_0,l_b) := \int_0^\infty \int_0^\infty u^a_{l_1}(k_1 r_1) u^b_{l_2}(k_2 r_2) \times \frac{r_<^\lambda}{r_>^{\lambda+1}} u^0_{l_0}(k_0 r_1) w_{l_b}(r_2) r_1^2 r_2^2 dr_1 dr_2 . \tag{13}$$

For high l states the fast incoming and outgoing electrons no longer penetrate the atom and a Bethe approximation to the radial matrix element becomes justified. In this case the integral (13) reduces to

$$I(l_1,l_2,\lambda,l_0,l_b) = I_{0,R}(l_1,l_2,\lambda,l_0,l_b) + B_{0,\infty}(l_2,\lambda,l_b) J_{0,\infty}(l_1,\lambda,l_0), \tag{14}$$

where we have defined

$$I_{0,R}(l_1,l_2,\lambda,l_0,l_b) := \int_0^R r_1^2 u^a_{l_1}(k_1 r_1) u^0_{l_0}(k_0 r_1) dr_1 \times \left[\frac{1}{r_1^{\lambda+1}} \int_0^{r_1} r_2^{\lambda+2} u^b_{l_2}(k_2 r_2) w_{l_b}(r_2) dr_2 + r_1^\lambda \int_{r_1}^\infty dr_2 r_2^{-\lambda+1} u^b_{l_2}(k_2 r_2) w_{l_b}(r_2) \right], \tag{15}$$

$$J_{0,\infty}(k_1,l_1,k_0,l_0,\lambda) := \int_R^\infty r_1^{-\lambda+1} u^a_{l_1}(k_1 r_1) u^0_{l_0}(k_0 r_1) dr_1 , \tag{16}$$

$$B_{0,\infty}(l_2,\lambda,l_b) := \int_0^\infty r_2^{\lambda+2} u^b_{l_2}(k_2 r_2) w_{l_b}(r_2) dr_2 . \tag{17}$$

The parameter R is the outer limit to which the solution of the differential equation will be integrated. The paper [29] deals extensively with the evaluation of these integrals so that we merely summarize the results here. Both electrons only see an atom potential and are asymptotically essentially free. This means that the distorted waves $u^a_{l_1}(k_1 r_1)$ and $u^0_{l_0}(k_0 r_1)$ can be approximated by Bessel functions resem-

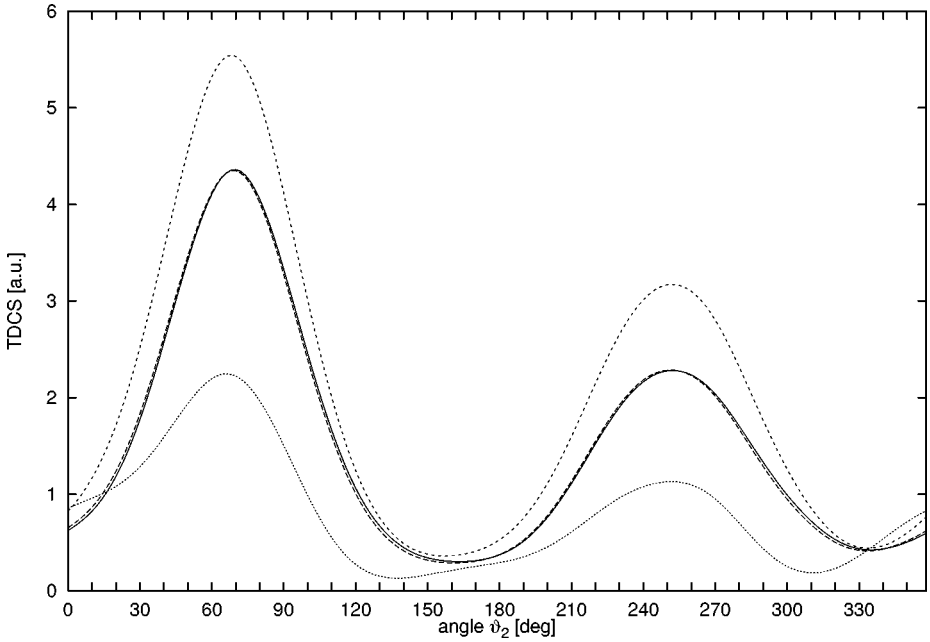

FIG. 5. TDCS of xenon $(5p)$ at an impact energy of 1032.8 eV, energy of slow outgoing electron is 20 eV, fast electron fixed at an angle of $\vartheta = 2.5°$. Comparison of the different stages of the convergence is made. Shown is DWBA using the triplet exchange potential for the slow outgoing electron and using $l = 400$ l states for fast incoming and outgoing electron (solid curve), using $l = 200$ (long dashed), using $l = 80$ (short dashed), and using only $l = 40$ (dotted). Number of l states for the slow outgoing electron is 15.

bling this free behavior for high l values. The integral over these two Bessel functions can now be solved analytically [30]. The analytic solution is a finite sum over associated Legendre functions of the second kind with the argument $\chi := (k_0^2 + k_1^2)/(2k_0k_1)$. Because k_0 and k_1 are nearly equal in this geometry χ goes to 1 and we are approaching the pole of the Legendre function. This means that more and more l states are contributing to the scattering event (in the unphysical limit χ would be equal to 1 and an infinite number of these l states would contribute).

The worst case for evaluating these integrals would be if we replaced all distorted waves by plane waves. Getting the TDCS to converge for this situation not only tests the accuracy of the integration routine but also the overall accuracy of the angular momentum algebra and the differential equation solver. The numerical methods used here were tested extensively by Rasch and Whelan [29], who were able to reproduce the analytic result available for hydrogen for the case of $E_0 = 1000$ eV, $E_1 = 985.4$ eV, $E_2 = 1$ eV to better than 1%. Note that these energies are even more extreme than the ones we have to consider here. Up to $l = 1000$ l states were needed for the convergence. In the case considered here we achieved convergence for little more than $l = 400$. In Fig. 5 we give a comparison for different converged results for xenon $(5p)$. Although merely $l = 10$ l states were needed for the slow outgoing electron (we used $l = 15$ to be safe) we do not get a converged result for $l = 80$ for the fast incoming and outgoing electron both calculated in the triplet potential of the ion. At about $l = 80$ the numerically calculated phase shifts are zero within the numerical accuracy so that the Bethe approximation becomes fully justified. Within the Bethe approximation we have retained the monopole, dipole, and quadrupole partial wave integral. Higher-order integrals can be neglected. However, we were surprised to see that especially for the hydrogen case even the quadrupole term gave a significant contribution to the cross section [29]. At about $l = 200$ for the fast incoming and outgoing electron the cross section is almost indistinguishable from a calculation using $l = 400$ l states.

B. Photoionization cross sections

By relating the TDCS to photoionization cross sections we have to make sure that theoretical photoionization cross sections using Hartree-Fock–based wave functions reproduce experimental measurements. This not only checks the program but also tests the quality of the wave function used. We remark that they were generated using a variational principle in order to minimize the energy of the atomic system (see [31]); it is therefore not obvious how these wave functions can reproduce other properties of the system. This is especially important in our case where the energy of the slow electron is close to the ionization threshold and significant deviations from the photoionization cross sections can be expected. However, since the Hartree-Fock wave functions are convoluted with the distorted wave of the slow outgoing electron we can only indirectly test the bound-state wave functions. We therefore test the quality of the distorted waves at the same time. The derivation of the photoionization cross sections for our Hartree-Fock wave functions can be found elsewhere [15].

We remark at this point that for xenon the use of Hartree-Fock rather than Dirac-Fock wave functions may lead to some error (see [32]). However, we do not envisage that the use of Hartree-Fock wave functions will give rise to a significant error in the absolute size of the triple-differential cross section.

In Tables II and III we compare the experimentally found values for β and the photoionization cross section $\sigma := d\sigma/dE$ with the theoretical ones. We find very good

TABLE IV. Comparison of the values for the limit determined experimentally and from the DWBA calculation using different forms of the local exchange potential for the slow outgoing electron.

	Kr $(4p)$	Xe $(5p)$
$\sigma_{\rm lim}$ exp.	1.01	0.387
$\sigma_{\rm lim}$ DWBA	0.371	0.348

agreement with the experimental β values for krypton and xenon. However, there is a very significant difference for the σ values in the case of krypton. Whilst the theoretical value of σ for the calculation for xenon is to within 11% of the experiment we get more than a factor of 2 for krypton.

In Table IV we compare the value of the limit given by Eq. (8) for experimental and theoretical data. We find again that the limit for xenon is to within 11% of the experiment while we get a factor of 2 difference for krypton. This discrepancy is clearly coming from the difference in the photoionization cross sections.

C. What else can go wrong?

Although there can be a large discrepancy between theory and experiment for the photoionization cross section as encountered in the case of krypton where theory and experiment disagree by a factor of 2, it does, however, not explain why the DWBA is a factor of 4–6 smaller for krypton. This is particularly the case for xenon where the disagreement between the photoionization cross sections is a mere 11% and not a factor 3–4. In the following sections we will first discuss the normalization of helium before we discuss it for krypton and xenon.

VI. THE NORMALIZATION OF HELIUM, KRYPTON, AND XENON

As we noted earlier agreement between the absolute size of the experimental data on He of [9] and our DWBA calculations is very good. However, we are finding large discrepancies when we apply the same method of normalization for krypton and xenon. In this section we will analyze in depth where this discrepancy arises and we will show that while the extrapolation technique is valid for helium it fails for the heavier elements.

A. Helium

We have recalculated some of the helium data taken at an impact energy of 600 eV [9]. In Fig. 6 we show a comparison between the absolute experimental data and our DWBA calculation. Figure 6 also shows a first Born calculation using the triplet potential for the slow outgoing electron. Good agreement is found. It is important to note that the difference between the DWBA and the first Born calculation is generally rather small.

1. The fitting of the helium data

As we remarked earlier Klar *et al.* [17] used only even powers in the expansion of the OOS. Even without this limi-

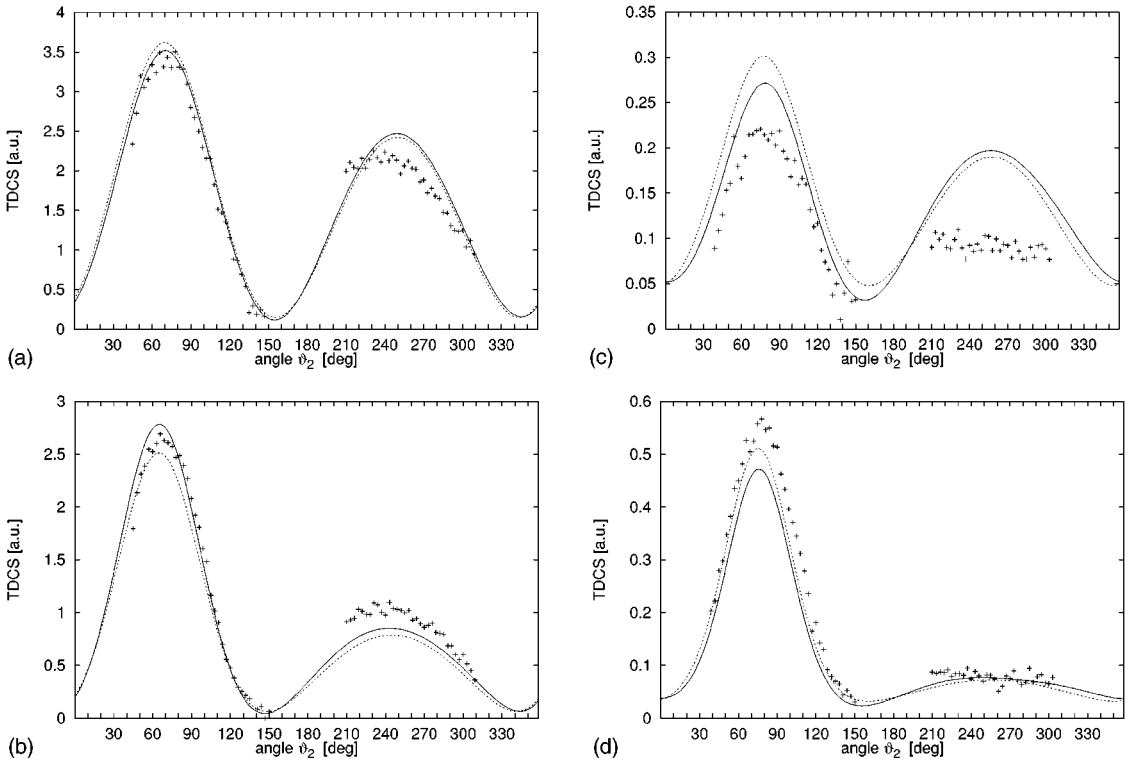

FIG. 6. TDCS of helium $(1s)$ in coplanar asymmetric geometry at an impact energy of 600 eV. Shown is the DWBA (solid curve) and first Born calculation (short dashed). Energy of slow outgoing electron is either 2.5 eV with angle of fast electron fixed at $\vartheta_1=4°$ (upper left) and $\vartheta_1=10°$ (upper right) or 10 eV with angle of fast electron fixed at $\vartheta_1=4°$ (lower left) and $\vartheta_1=10°$ (lower right). Experimental data are on an absolute scale and given in a.u.

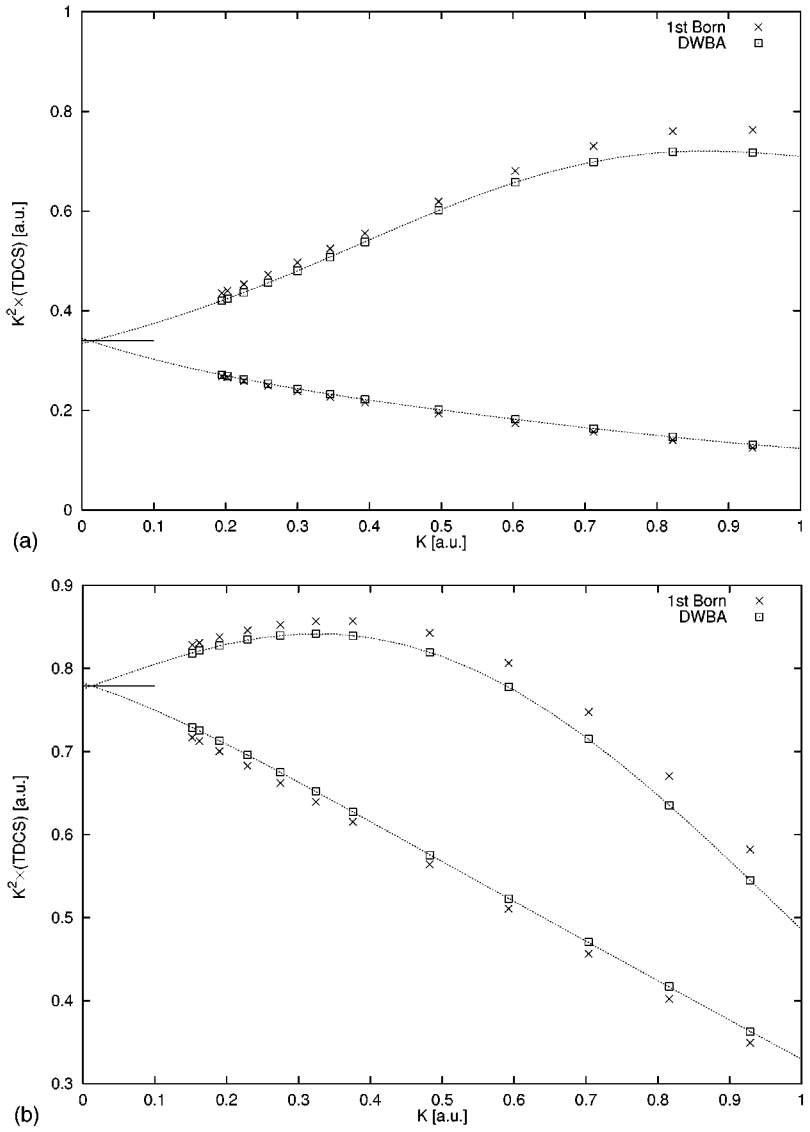

FIG. 7. The limiting process of helium ($1s$) at an impact energy of 600 eV, the energy of slow outgoing electron is 10 eV (above) and 2.5 eV (below). Shown is TDCS multiplied with the square of the momentum transfer $K^2=|\boldsymbol{k}_0-\boldsymbol{k}_1|^2$ against K. We compare the first Born calculation (crosses) with the DWBA (squares) calculations. The horizontal bar at 0.340 (above) and at 0.779 (below) denotes the analytic limit of the first Born calculation.

tation we found that the fitting of the theoretical curves especially the first Born curves were very stable and accurate indeed. In Fig. 7 we show the first Born and DWBA calculation and an extrapolation to the zero-momentum transfer. As can be seen the first Born and DWBA results are very close together over a wide range of K values. Especially close to the unphysical region the two theories are almost indistinguishable so that Lassettre's theorem, which depends crucially on the applicability of the first Born approximation, can indeed be used. We were able to reproduce the limit as given in Eq. (8) from the extrapolation of the first Born points to 4 digits (this limit is indicated by a short horizontal bar in Fig. 7). The extrapolation of the DWBA was slightly less accurate and stable. We could, however, reproduce the limit for most polynomials to better than 5%.

Due to the experimental setup there was a rather large gap between the region of K, which is accessible to experiment, and $K=0$ the extrapolation point. In order to obtain reliable results Jung *et al.* [9] chose a narrow spacing of ΔK and performed the measurements with high statistical accuracy. They remark that the error of the extrapolation procedure is smaller than 10%.

B. Krypton and xenon

We have seen that the DWBA is very well capable of reproducing the absolute cross sections in the case of helium. Furthermore the limiting process is justified as the DWBA has gone over to the first Born approximation which validates Lassettre's theorem. In the following sections we will discuss the fitting procedure for the experimental and theoretical curves for krypton and xenon.

C. The fitting of the experimental data

We have used a fitting procedure as described in the section above about the normalization of helium. Although the gap between the experimentally accessible region and the extrapolation point at $K=0$ is about 0.25 and therefore much

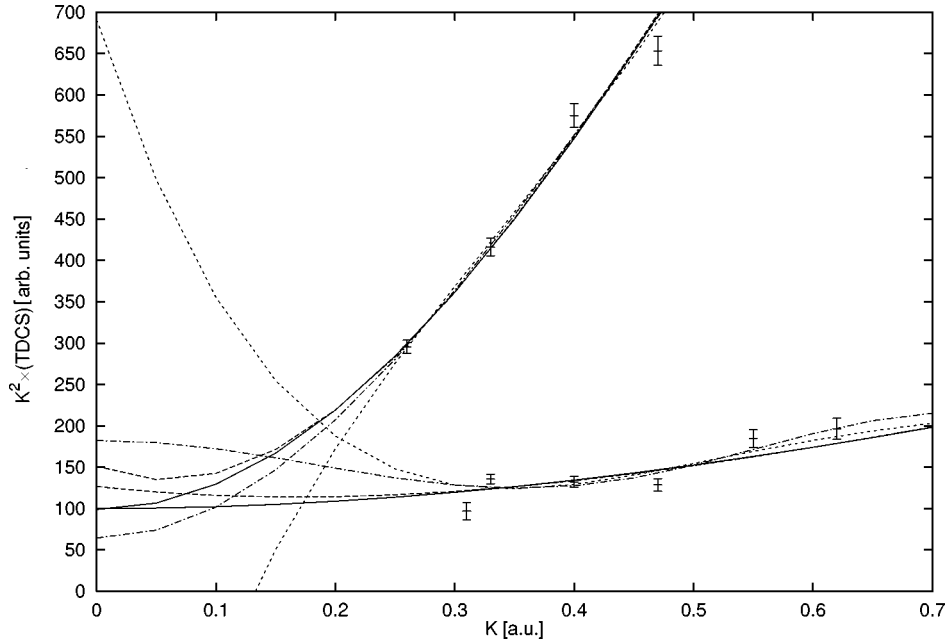

FIG. 8. The limiting process of xenon $(5p)$ at an impact energy of 1032.8 eV, the energy of slow outgoing electron is 20 eV. Shown is the experimentally determined TDCS multiplied with the square of the momentum transfer $K^2=|\boldsymbol{k}_0-\boldsymbol{k}_1|^2$ against K. We compare different polynomial fits: fourth-order polynomial including only even terms (solid curve), third-order polynomial (long dashed), fourth-order polynomial (short dashed), eighth-order polynomial including only even terms (dashed dotted). The minimum K value at $\vartheta_1=0°$ is $K=0.139$.

smaller than in the helium case (about 0.5) the experimental data points are rather scarce and more scattered. In Fig. 8 we show the results of the fitting for the experimental curves for a variety of polynomials. We find that there is only a very limited range of polynomials that give a reasonable fit and produces the same extrapolation value of the ordinate for the binary and recoil curve. In particular we found that using only an even polynomial and fitting it to the fourth, sixth or eighth order produced a similar limiting point for the binary and recoil curve. We encountered similar problems in the krypton case (not shown).

D. The fitting of the theoretical data

We have performed a similar fitting for the theoretical curves to determine the limit. In Figs. 9 and 10 we compare the limiting procedure for a first Born and the DWBA calculation with the experimental data for krypton and xenon. We have scaled the experimental data to give the best agreement with the binary curve of the DWBA calculation. We found again, similar to the helium case, that the fitting procedure for the first Born curve is very stable and reproduces the limiting point as given in Eq. (8). However, the DWBA disagrees with the first Born approximation over a wide range and converges to the first Born approximation only very closely to the unphysical region if not inside. It is therefore probably not too surprising that the extrapolation of the DWBA does not converge to the same point at $K=0$. One can only conclude from a theoretical point of view that the distortion effects are still too strong and a first Born treatment as required by Lassettre's theorem is not justified.

The difference between the experimentally obtained limit and the first Born limit given by Eq. (8) disagree by more than a factor of 2.5. Unfortunately, the case of krypton is more ambiguous. As we have already seen the photoionization cross sections are not well reproduced and indeed the experimental data seem to lie between the DWBA and the first Born results (see Fig. 10). However, we note that for krypton the DWBA converges to the first Born limit only very close to the unphysical region and that both curves tend to bend rather strongly.

VII. CAN THE DIFFICULTIES BE OVERCOME?

If we compare the Figs. 7 with 9 and 10 we see that the most striking difference lies in the fact that there is almost no difference of the DWBA and the first Born calculation in the helium case whereas for krypton and xenon both calculations are very different over a wide range and only start to merge very close to the unphysical region. Although any theory has to converge to the first Born eventually this can happen very deep inside the unphysical region. This is indeed the case for the DWBA and is also reflected in the slightly unstable extrapolation of the DWBA to the $K=0$ limit.

Another important point related to the previous finding is that the fitting curves do not exhibit a stable extrapolation behavior (see Fig. 8). We would note two points: Firstly, to have a more reliable extrapolation we would need very many more experimental points. Secondly, fitting the theoretical curves indicates that we do not reach the region of applicability of Lassettre's theorem until well inside the unphysical region. This would indicate that such extrapolation techniques are doomed to fail.

VIII. CONCLUSION

A new set of TDCS for Kr and Xe have been measured and compared with DWBA calculations. We have considered the extrapolation technique used in [9] and attempted to place the experimental data on an absolute scale. A satisfac-

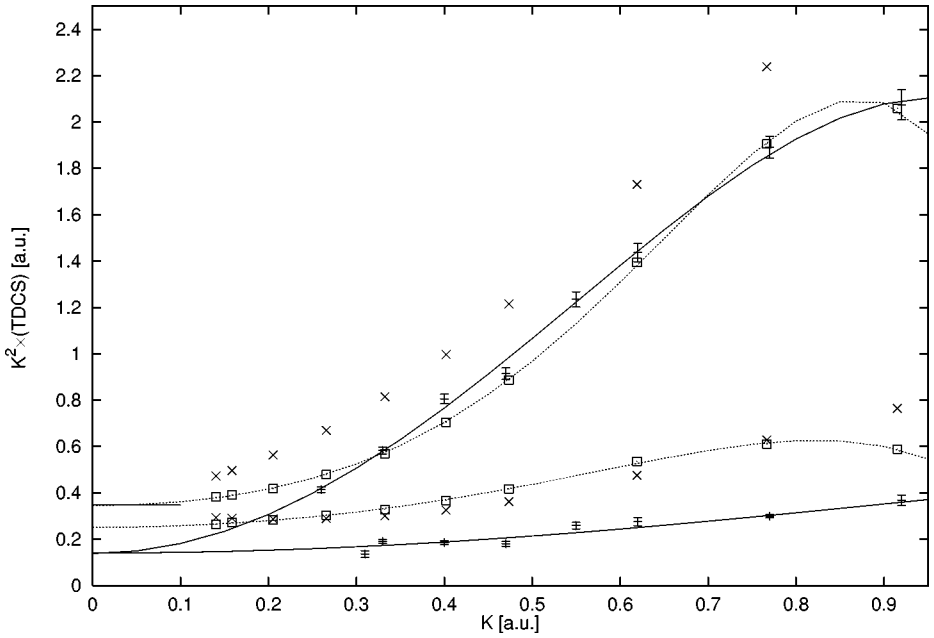

FIG. 9. The limiting process of xenon $(5p)$ at an impact energy of 1032.8 eV, the energy of slow outgoing electron is 20 eV. Shown is TDCS multiplied with the square of the momentum transfer $K^2=|\boldsymbol{k}_0-\boldsymbol{k}_1|^2$ against K. We compare the first Born (crosses) with the DWBA (squares) calculations and the experimental data, which was scaled to give the best fit to the binary peak. Shown are a polynomial fit to the experiment (solid curve) and to the DWBA calculation (dotted line). The horizontal bar at 0.3475 denotes the analytic limit of the first Born calculation. The minimum K value at $\vartheta_1=0°$ is $K=0.139$.

tory agreement, at least in regard to shape, between theory and experiment has been found. Especially in the binary region and for larger scattering angles of the fast outgoing electrons ($\vartheta_1=8°$ for krypton and xenon) we get very good shape agreement with experiment; this is the region where the first Born approximation does rather poorly. However, a large discrepancy between the absolute size of the cross sections deduced from the extrapolation technique and the calculated results exist. This discrepancy has triggered an extensive investigation of its origin. We have demonstrated that

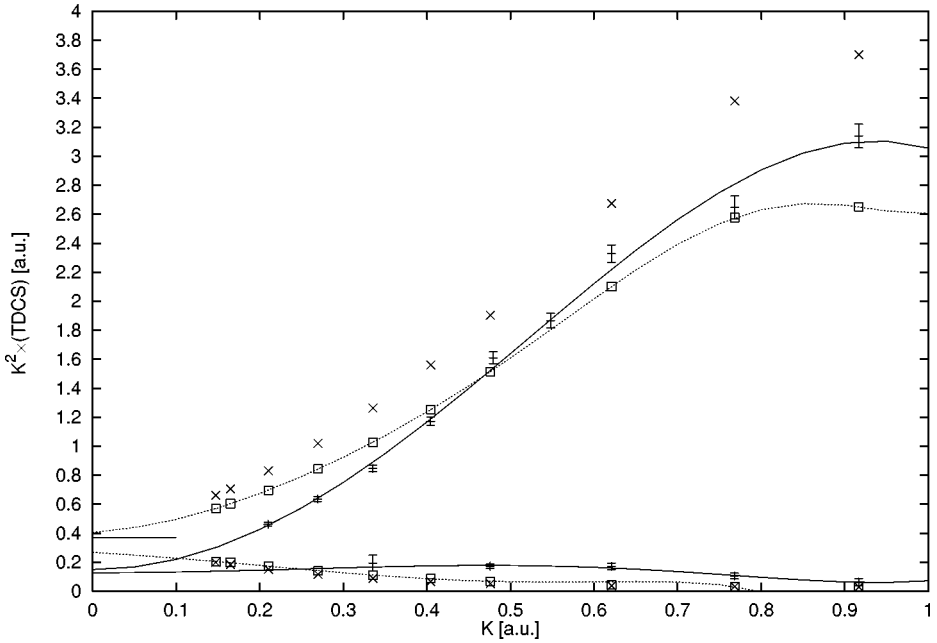

FIG. 10. The limiting process of krypton $(4p)$ at an impact energy of 1034.5 eV, the energy of slow outgoing electron is 20 eV. Shown is TDCS multiplied with the square of the momentum transfer $K^2=|\boldsymbol{k}_0-\boldsymbol{k}_1|^2$ against K. We compare the first Born calculation (cross sign) with the DWBA (squares) calculations and the experimental data, which was scaled to give the best fit to the binary peak. Shown are a polynomial fit to the experiment (solid curve) and to the DWBA calculation (dotted line). The horizontal bar at 0.3714 denotes the analytic limit of the first Born calculation. The minimum K value at $\vartheta_1=0°$ is $K=0.147$.

the extrapolation technique used in [9] would appear to be valid for helium, but is questionable for the heavier atoms in the kinematics investigated in this experiment. The good agreement in shape together with the consistency in absolute size for helium encourages one to view the DWBA as a suitable theoretical approximation in these very asymmetric geometries. However, it has to be emphasized that the main conclusion of this paper is that one may only use the extrapolation technique for heavy atoms with extreme caution if at all, since the distortion effects of the heavy nuclei makes it difficult to experimentally access that region where Lassettre's theorem might be usefully exploited. A second problem lies in the instability of the fitting procedure itself. It is to be doubted that this instability could be removed by a set of data with better measurement statistics and more data points close to the unphysical region since our calculations indicate that the theoretical curves have not attained their limiting behavior at the boundary of the unphysical region.

ACKNOWLEDGMENTS

We gratefully acknowledge financial support for this work by the British Council and DAAD (ARC), NATO, through Grant CRG 950407 and the European Union (HCM CHRX-CT93-0350). J.R. would like to thank Wolfson College, Cambridge for financial support. M.Z. is indebted to the Slovenian Ministry of Science and Technology for supporting his stay in Rome. This work was completed while C.T.W. was supported by the NSF as a visitor at the Institute of Theoretical Atomic and Molecular Physics at Harvard University and Smithsonian Astrophysical Observatory. We are grateful to Professor J. H. Macek for some very helpful discussions.

[1] G. Stefani, L. Avaldi, and R. Camilloni, J. Phys. C **6**, 1 (1993).
[2] C. T. Whelan, R. J. Allan, H. R. J. Walters, and X. Zhang, in (2,2*e*) *and Related Processes,* edited by C. T. Whelan, H. R. J. Walters, A. Lahmam-Bennani, and H. Ehrhardt (Kluwer Academic Publisher, Dordrecht, 1993), p. 1.
[3] M. Inokuti, Rev. Mod. Phys. **43**, 297 (1971).
[4] H. R. Walters, X. Zhang, and C. T. Whelan, in (*e,2e*) *and Related Processes* (Ref. [2]), p. 33.
[5] G. Ehrhardt, H. Knoth, P. Schlemmer, and K. Jung, Z. Phys. D **1**, 3 (1986).
[6] A. Lahmam-Bennani, M. Cherid, and A. Duguet, J. Phys. B **20**, 2531 (1987).
[7] G. Stefani, R. Camilloni, and A. Giardini-Guidoni, Phys. Lett. **64A**, 364 (1978).
[8] B. van Wingerden, J. J. N. Kimman, M. van Tilburg, and F. J. de Heer, J. Phys. B **14**, 2475 (1981).
[9] K. Jung *et al.*, J. Phys. B **18**, 2955 (1985).
[10] E. Fainelli, R. Camilloni, G. Petrocelli, and G. Stefani, Nuovo Cimento D **9**, 33 (1987).
[11] L. Avaldi *et al.*, Phys. Rev. A **48**, 1195 (1993).
[12] A. Lahmam-Bennani, H. F. Wellestein, A. Duguet, and M. Lecas, Rev. Sci. Instrum. **56**, 43 (1985).
[13] Y.-K. Kim, Phys. Rev. A **28**, 656 (1983).
[14] E. N. Lassettre, A. Skerbele, and M. A. Dillon, J. Chem. Phys. **50**, 1829 (1969).
[15] J. Rasch, Ph.D. thesis, University of Cambridge, 1996.
[16] W. H. Press, S. A. Teukolsky, W. T. Vetterling, and B. P. Flannery, *Numerical Recipes in Fortran* (Cambridge University Press, Cambridge, 1992).
[17] H. Klar, K. Jung, and H. Ehrhardt, Phys. Rev. A **29**, 405 (1984).
[18] J. Furness and I. McCarthy, J. Phys. B **6**, 2280 (1973).
[19] S. Ward and J. Macek, Phys. Rev. A **49**, 1049 (1994).
[20] C. T. Whelan *et al.*, Phys. Rev. A **50**, 4394 (1994).
[21] J. Röder *et al.*, Phys. Rev. A **53**, 225 (1996).
[22] Y. V. Popov and J. J. Benayoun, J. Phys. B **14**, 4673 (1981).
[23] H. Klar, A. Franz, and H. Tenhagen, Z. Phys. D **1**, 373 (1986).
[24] F. W. Byron and C. J. Joachain, Phys. Rep. **4**, 212 (1989).
[25] A. Fahlman, M. O. Krause, T. A. Carlson, and A. Svensson, Phys. Rev. A **30**, 812 (1984).
[26] S. Aksela *et al.*, Phys. Rev. A **36**, 3449 (1987).
[27] M. O. Krause, T. A. Carlson, and P. R. Woodruff, Phys. Rev. A **24**, 1374 (1981).
[28] S. H. Southworth *et al.*, Phys. Rev. A **24**, 2257 (1981).
[29] J. Rasch and C. T. Whelan, Comput. Phys. Commun. **101**, 31 (1997).
[30] C. T. Whelan, J. Phys. B **26**, 2343 (1985).
[31] E. Clementi and C. Roetti, At. Data Nucl. Data Tables **14**, 177 (1974).
[32] J. P. D. Cook, J. Mitroy, and E. Weigold, Phys. Rev. Lett. **13**, 1116 (1984).